Supporting Information for

Hg(II)-causes Photoluminescence Quenching of Pyrene inside a Blue Emitting Ionic Liquids Derived Crystalline Nanoball

Najmin Tohora[a], Rajkumar Sahoo[b], Sabbir Ahamed[a], Jyoti Chourasia[a], Shubham Lama[a], Manas Mahato[a], Shreya Ali[a] and Sudhir Kumar Das[a*]

[a]Department of Chemistry, University of North Bengal, Raja Rammohunpur, Darjeeling, West Bengal-734013, India

[b]Department of Chemistry, Indian Institute of Technology, Kharagpur, West Bengal-721302, India

Corresponding author: (Dr. S. K. Das; E-mail: sudhirkumardas@nbu.ac.in)

Table of Contents

S.1 Preparation of NTIL and nNTIL

For the preparation of **NTIL**, we first synthesized sodium salt of pyrene butyrate (PBNa) by simply treating the pyrene butyric acid with an equivalent amount of NaOH in methanol, and the mixture was stirred for 6 hours. After evaporating the solvent, yellow color solid PBNa was obtained. **NTIL** was synthesized by using previously described procedures with a few modifications[1]. Briefly, PBNa and the ionic liquid $P_{66614}Cl$ were taken in a 1:1 molar ratio in a dichloromethane (DCM)-water mixture of 2: 1 (v/v) ratio. The mixture was stirred throughout the night. The color of the bottom layer (DCM layer) was shifted from colorless to pale yellow, and the upper layer (water layer) turned colorless, signifying that the ion exchange procedure had been successful. The water layer was removed, and the DCM layer was repeatedly washed with water to eliminate the by-product NaCl. The elimination of NaCl was verified using $AgNO_3$ solutions and washing the reaction mixture several times until there was no longer any white precipitate resulting from the production of AgCl.The trace amount of water in the DCM layer containing **NTIL** is removed by passing it through the anhydrous Na_2SO_4. By evaporating DCM and the remaining water under vacuum at ~60 °C for 2 hours, **NTIL** is obtained **(Scheme S1).** The synthesized **NTIL** was then characterized by NMR, HRMS, FTIR, and UV-visible absorption and emission spectral analysis. By utilizing reprecipitation methods, the nano-GUMBOS **nNTIL** has been fabricated and characterized by various analytical techniques[2]. Very briefly, a stock solution of **NTIL** (1 mg/mL) was prepared in tetrahydrofuran (THF), a good solvent, by dissolving the required quantity of **NTIL** in THF. The formation of aqueous suspended nanoparticles with varying (net) concentrations was achieved by rapidly injecting various aliquots of **NTIL** into the

water, followed by sonicating for around 30 minutes. The formation of nanoparticles,**nNTIL,** is confirmed by SEM, DLS, EDS**,** UV−visible absorption, and emission spectral analysis.

S.2 General Procedure for UV–visible and Fluorescence Experiments

The stock solutions of the sensor (4.9×10^{-5} M) and metal chloride solutions (1.0×10^{-3}M)were prepared in aqueous solution. Also, the metal and anions salts solutions (1.0×10^{-3}M) were prepared in an aqueous medium. The UV–visible and fluorescence response of various metal ions (Hg^{2+}, Sn^{2+}, Zn^{2+}, Cu^{2+}, Mn^{2+}, Ni^{2+}, K^{+}, Na^{+}, Pb^{2+}, Al^{3+}, Ba^{2+}, Ca^{2+} and Fe^{3+}) were investigated. The selectivity of the probe has been tested for all the metal ions using fluorescence experiments. To 2 mL of the sensor, 113 μM of each metal ion solution was introduced and stirred before carrying out fluorescence measurements. The fluorescence and UV–visible titrations were achieved by using varied concentrations of metal ion solution. The quantum yield (ϕ) of the sensor in the presence and absence of the mercury (II) ions has been calculated according to the formula [3].

S.3 Determination of fluorescence quantum yield

The quantum yield, Φ, was calculated by using the following equation:

$$\Phi = \Phi_s\left(\frac{F_x}{F_s}\right)\left(\frac{A_s}{A_x}\right)\left(\frac{{\eta_x}^2}{{\eta_s}^2}\right)$$

Where x & s indicate the unknown and standard solutions, respectively, Φ is the quantum yield, F is the area under the emission curve, A is the absorbance at the excitation wavelength, η is the index of refraction of the solvent. Φ measurements were performed using 4-aminophalimide in DMSO as standard (Φ=0.83)[3]. The estimated quantum yield for **nNTIL** is 0.37 and in the case of **nNTIL**-Hg^{2+}, the value is 0.035.

S.4 Preparation of portable paper-based test strips

The Whatman-41 filter paper is cut into strips, which are fully immersed in **nNTIL** aqueous solution (49 μM) for a while. Finally, the test strips are removed and dried in a hot

air oven at 60 °C. Some drops of all the metal ions solution (10^{-2} M) are added to these filter papers.

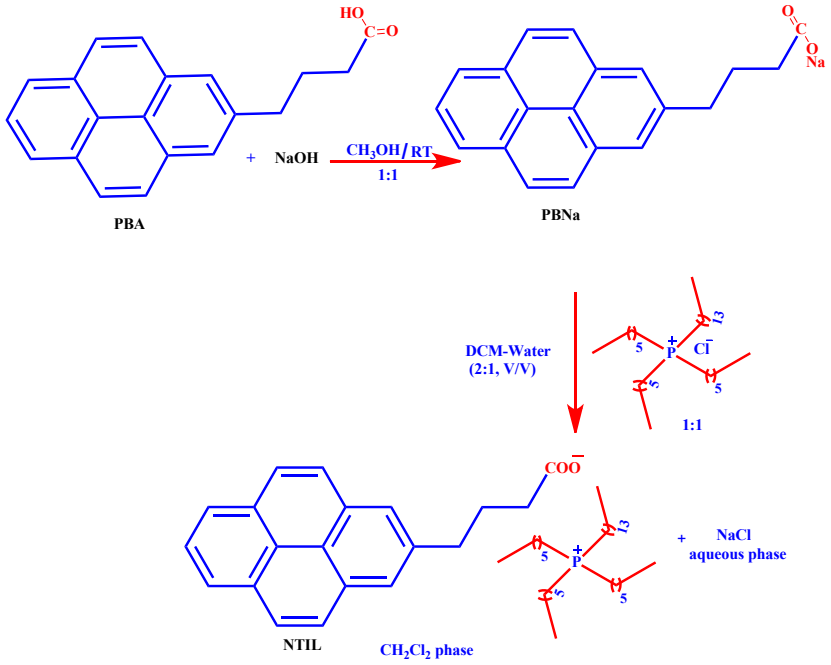

Scheme S1: Synthetic route for the preparation of **NTIL**.

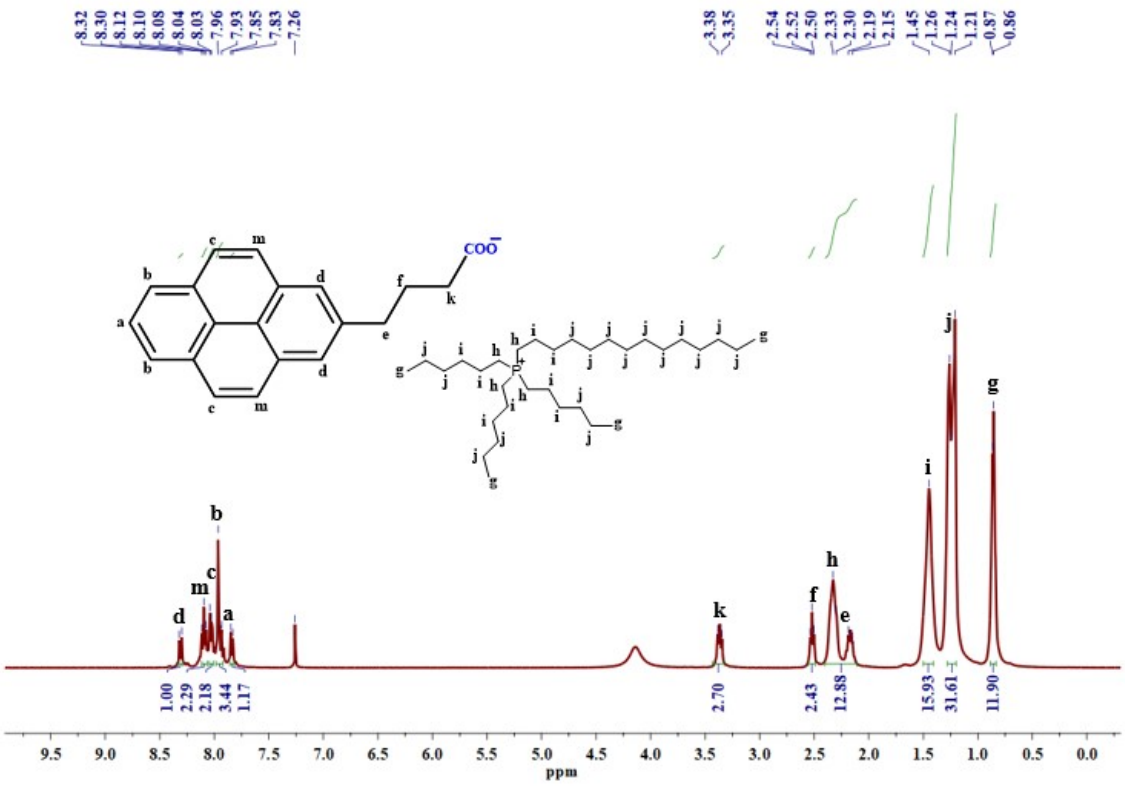

Fig. S1: ^{1}H NMR spectrum ($CDCl_3$, 400 MHz) of **NTIL**.

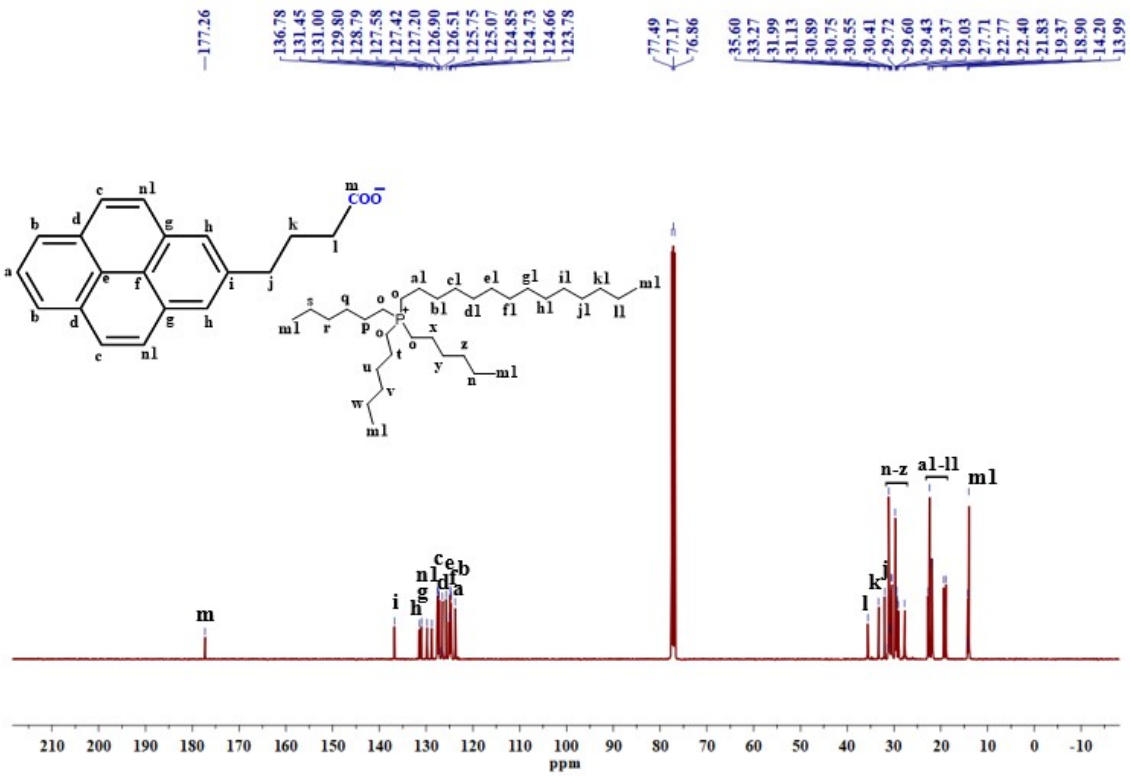

Fig. S2: ^{13}C NMR spectrum ($CDCl_3$, 100 MHz) of **NTIL**.

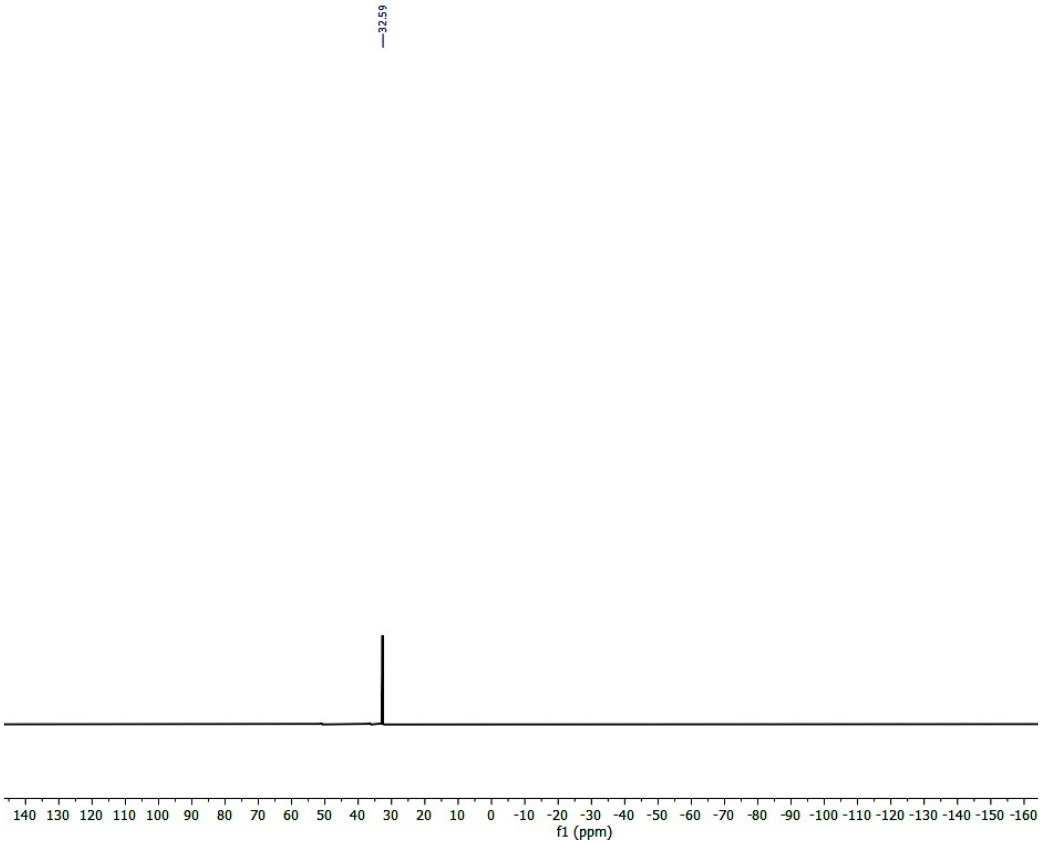

Fig. S3: ^{31}P NMR spectrum ($CDCl_3$, 400 MHz) of **NTIL**.

Trihexyl(tetradecyl)phosphonium 4-(pyrene-1-yl)butanoate (NTIL):

^{1}H NMR (400 MHz, $CDCl_3$, δ (ppm)): 8.31 (d, 1H), 8.10 (t, 2H), 8.06 – 8.02 (m, 2H), 7.96 – 7.93 (m, 3H), 7.85 (d, 73 1H), 3.39 – 3.35 (m, 2H), 2.52 (t, 2H), 2.38 – 2.35 (m, 8H), 2.21 – 2.24 (m, 2H), 74 1.57 – 1.39 (m, 16H), 1.28 – 1.22 (m, 32H), 0.88 – 0.86 (m, 12H).**^{13}C NMR** (100 MHz, $CDCl_3$, δ (ppm)): 177.3, 136.7, 131.5, 131.0, 129.9, 128.8, 127.6, 127.4, 127.3, 126.6, 126.5, 125.75, 125.07, 124.9, 124.7, 124.6, 123.8, 35.6, 33.3, 32.0, 31.2, 31.1, 30.8, 30.6, 30.5, 30.4, 29.7, 29.6,29.4, 29.3, 29.0, 27.7, 22.7, 22.4, 21.8, 19.4, 18.9, 14.2, 14.0, 13.9. **^{31}P NMR** (400 MHz, $CDCl_3$, δ (ppm): 32.59.

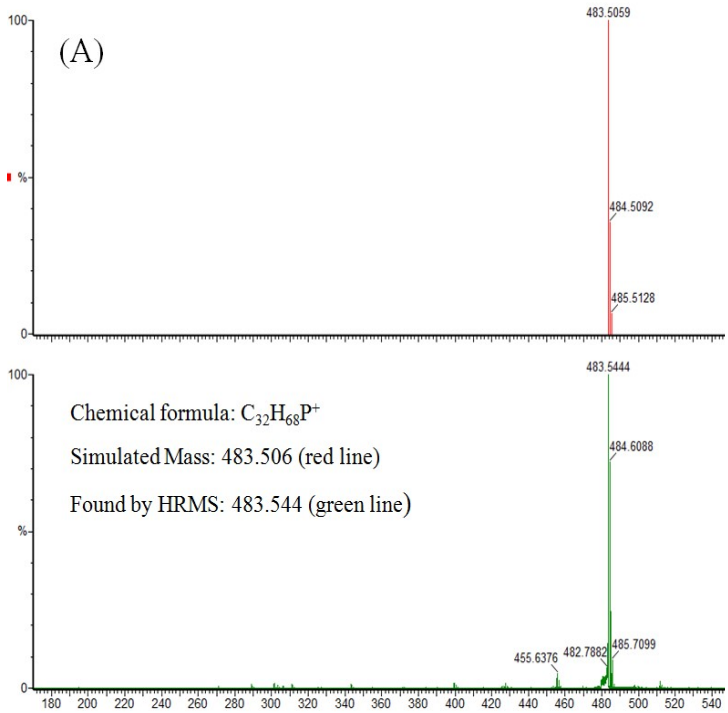

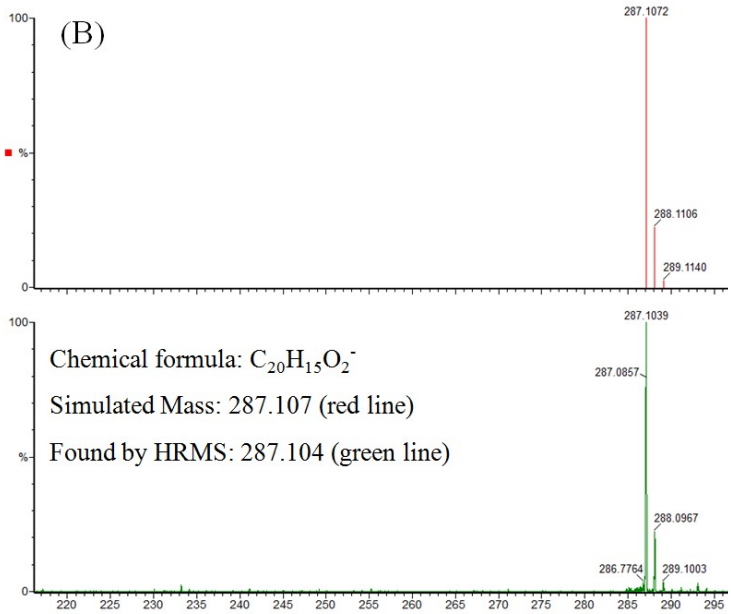

Fig. S4: HRMS spectra of **NTIL**; **(A)** positive ion mode and **(B)** negative ion mode.

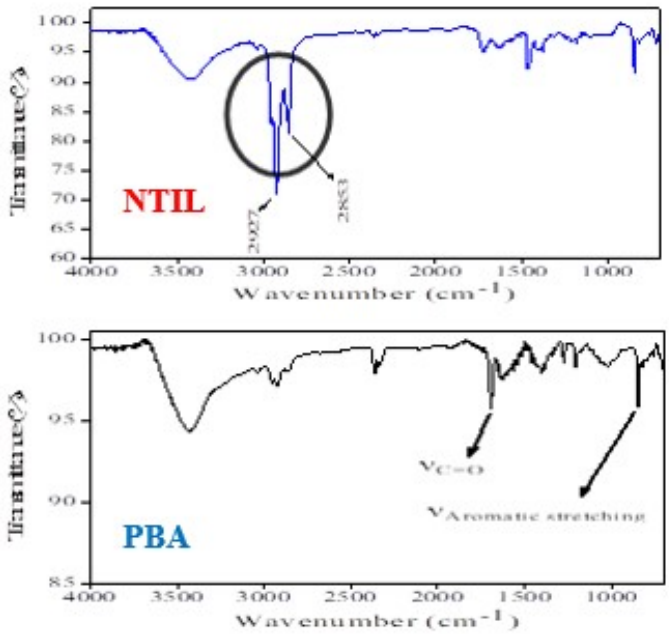

Fig. S5:FTIR spectra of pyrene butyric acid (PBA) (bottom) and **NTIL** (top).

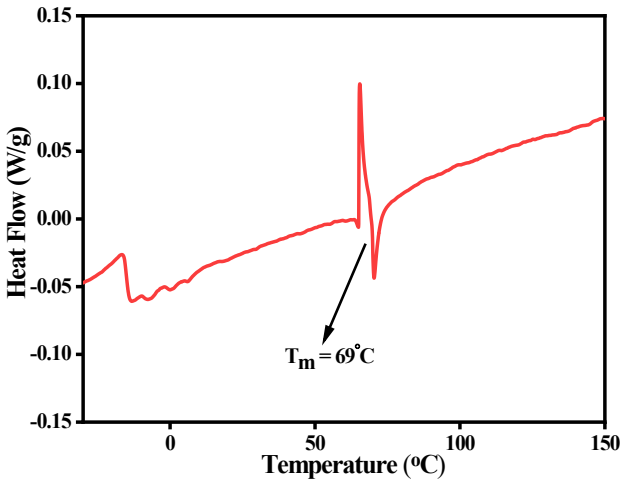

Fig. S6:DSC trace of **NTIL** ionic salt under nitrogen atmosphere. The scanning rate is 2 ºC min^{-1}.

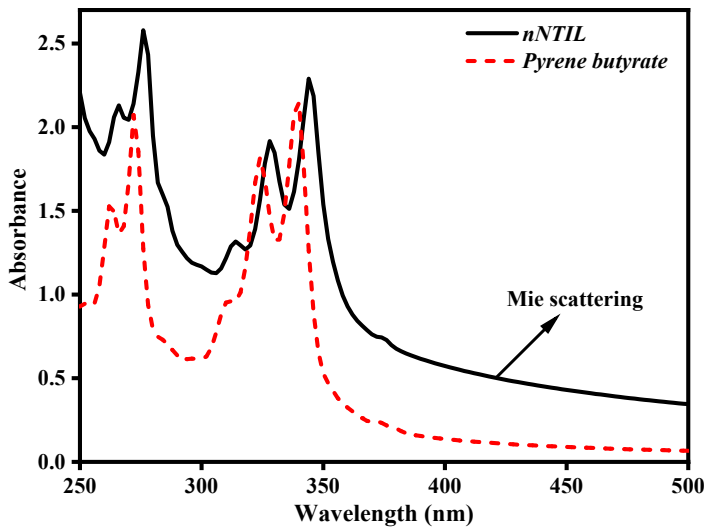

Fig. S7: Absorption spectra of pyrene butyrate and **nNTIL** in water.

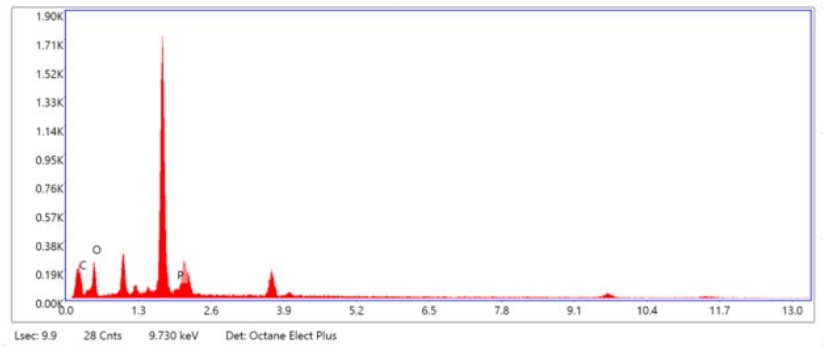

eZAF Smart Quant Results

Element	Weight %	Atomic %	Error %
C K	53.06	64.02	7.83
O K	32.00	28.99	11.49
P K	14.94	6.99	4.73

Fig. S8: Three kinds of element content and their weight and atomic percentages were shown in the case of **nNTIL**.

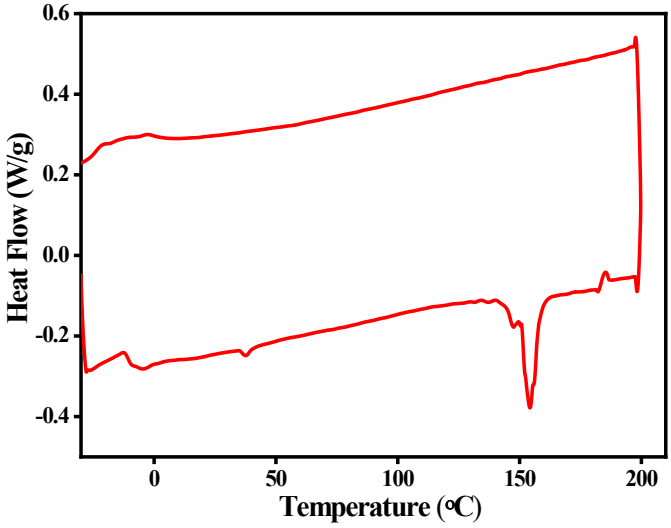

Fig. S9: DSC trace of **nNTIL** under nitrogen atmosphere. The scanning rate is 2ºC min^{-1}.

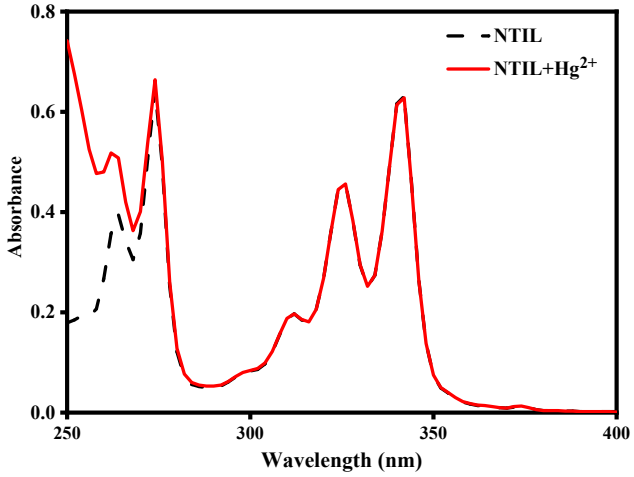

Fig. S10: Absorption spectra of **NTIL** in **NTIL**-Hg^{2+} in THF.

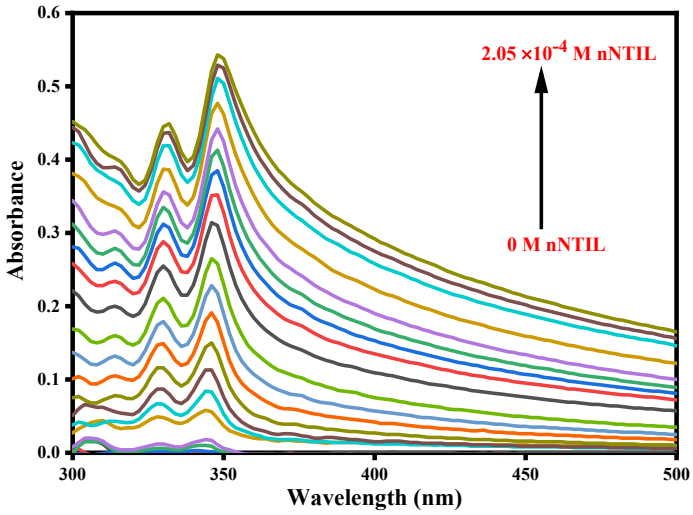

Fig. S11: Absorption spectra of Hg^{2+} with the addition of different concentration of **nNTIL.**

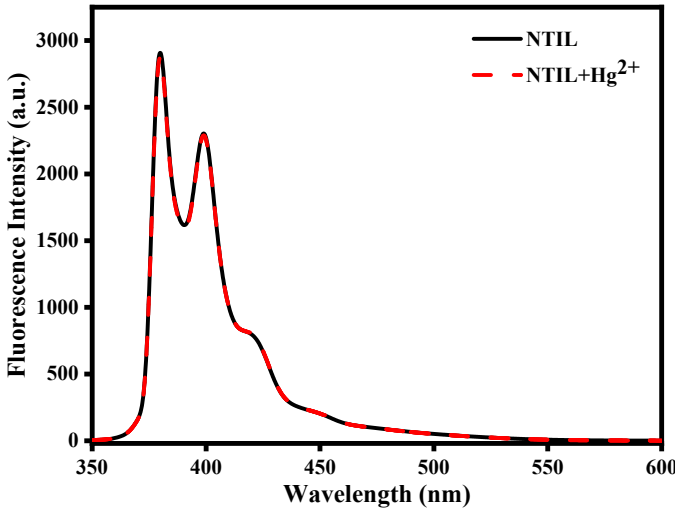

Fig. S12: Fluorescence spectra of **NTIL** in **NTIL**-Hg^{2+} in THF.

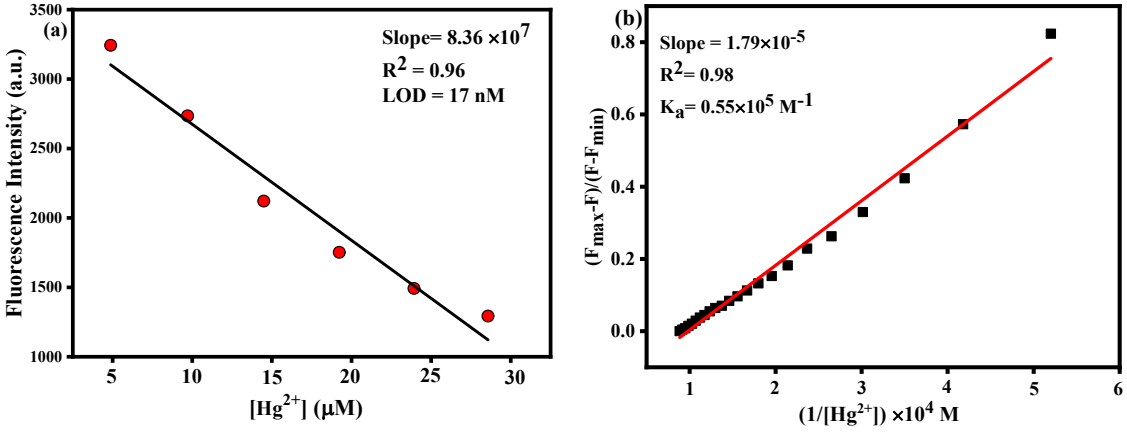

Fig. S13: (a) Calibration curve used to estimate the limit of detection (LOD). **(b)** Graph illustrating the binding affinity between **nNTIL** and Hg^{2+} ions.

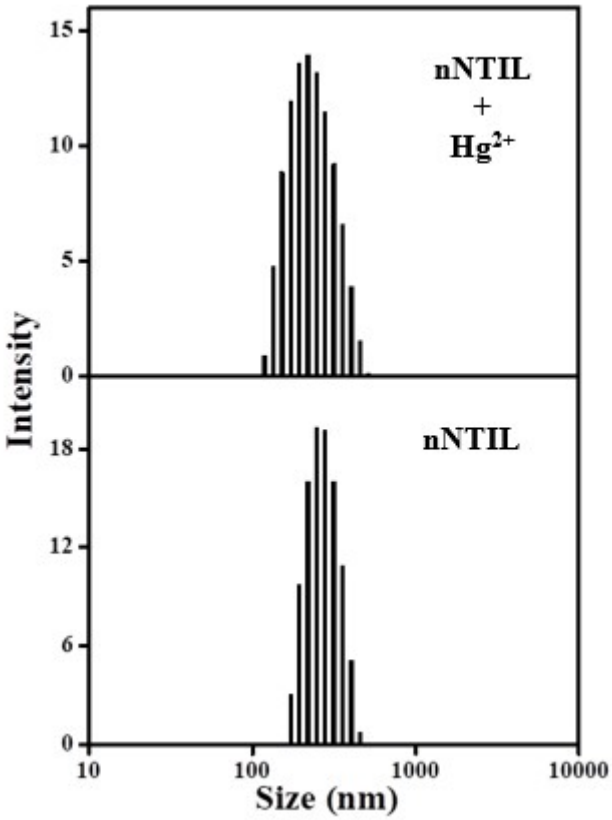

Fig. S14: DLS spectrum of **nNTIL** and **nNTIL**-Hg^{2+}.

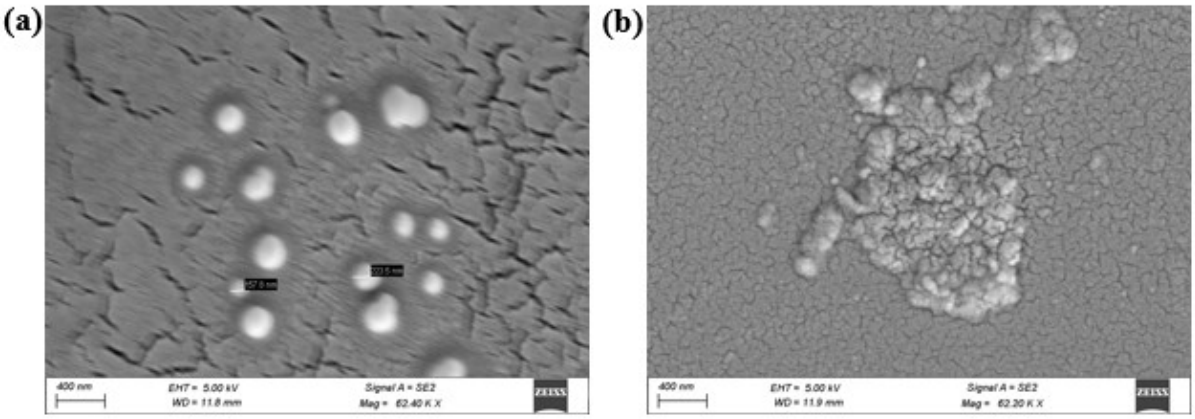

Fig. S15:SEM images of **nNTIL** and **nNTIL**-Hg^{2+}.

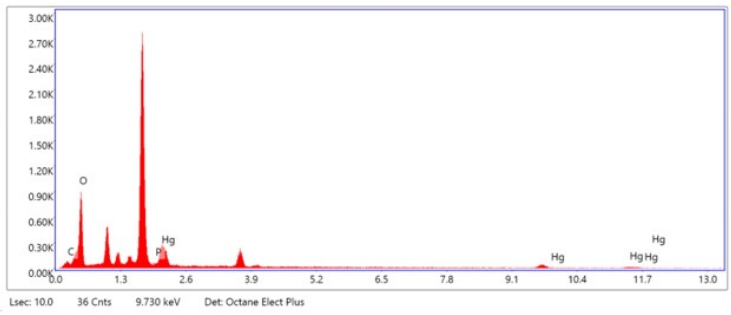

eZAF Smart Quant Results

Element	Weight %	Atomic %	Error %
C K	6.99	17.39	7.89
O K	39.55	73.83	6.04
P K	1.00	0.96	48.10
Hg L	52.46	7.81	21.82

Fig. S16: Four kinds of element content and their weight and atomic percentages were shown in the case of **nNTIL**-Hg^{2+}.

Table S1: Determination of Hg^{2+} in water samples.

Sample	Added (μM)	Found (μM)	Recovery (%)
Municipality water	9.70	9.67	99.69
	12.10	12.07	99.75
	14.49	14.46	99.79
	16.86	16.82	99.76
	19.23	19.17	99.68
	21.58	21.51	99.67
Tap water	9.70	9.52	98.14
	12.10	12.05	99.58

	14.49	14.39	99.30
	16.86	16.69	98.99
	19.23	19.15	99.58
	21.58	21.45	99.39

Table S2: Comparison with the detection limits of sensing Hg^{2+} ions by various sensors.

Sl. No	Sensor	Solvent	Detection Limit	Application	Ref.
1	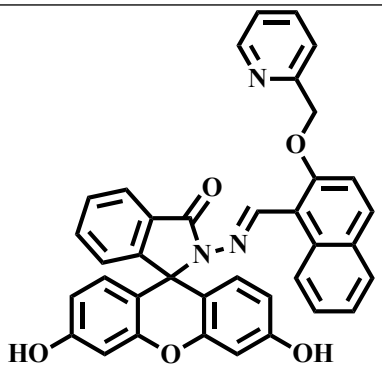	10 mM HEPES buffer	1.24 μM	Cell imaging	4
2	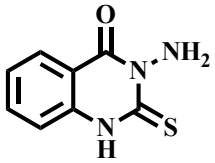	Aqueous media	0.35 μM	Metal ion sensor and real sample analysis	5
3	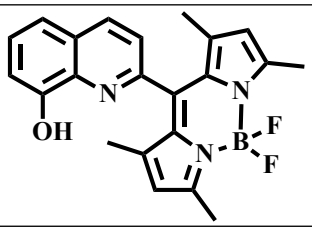	dioxane-water (1:3, v/v) solvent	5 μM	Metal ion sensor	6
4	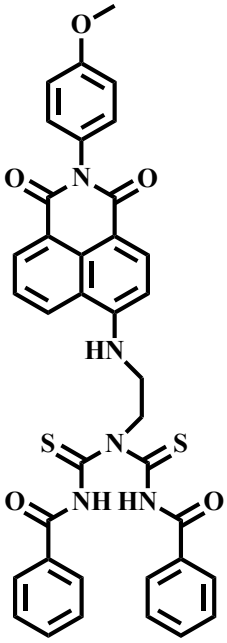	MeCN/H_2O (4/1, v/v)	0.83 μM	Cell imaging and water sample	7

5	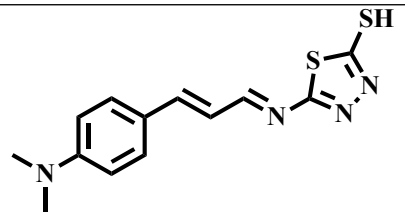	1:1 (v/v) acetonitrile/HEPES Buffer (10mM, pH 7.4)	2 μM	Water sample	8
6	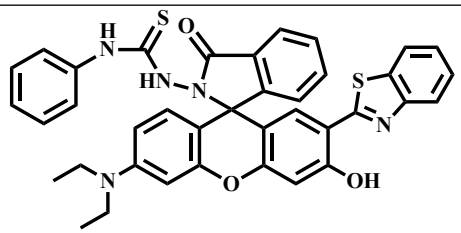	THF/HEPES (4:6, v/v, pH = 7.4) buffer solution	0.27 μM	Cell imaging	9
7	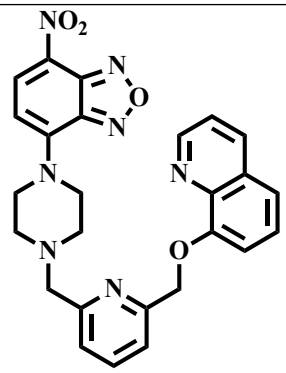	100 % aqueous solution	19.2 nM	Cell imaging	10
8	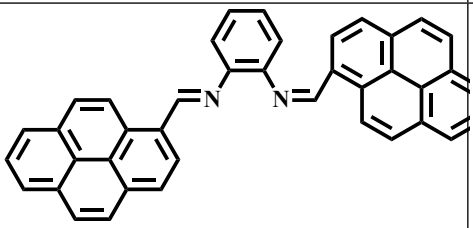	aqueous MeCN	90 nM	Cell imaging and test strip application	11
9	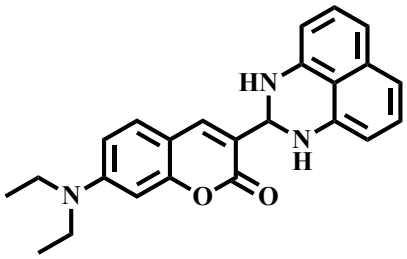	CH_3CN/H_2O (v/v = 3/7) solutions	1.08 μM	Bioimaging in living cells and zebrafish	12
10	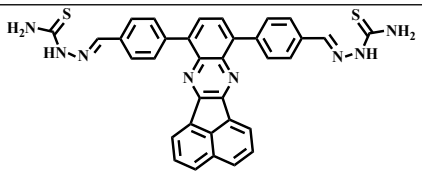	DMSO/H_2O (v/v=9/1) buffered by 50mMTris-HCl at pH=7.0.	0.90 μM	Water sample	13
11	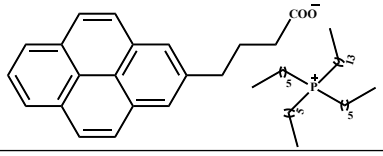	**100 % aqueous solution**	**17 nM**	**Water and soil samples**	**Our work**

References

1 W. I. S. Galpothdeniya, K. S. McCarter, S. L. De Rooy, B. P. Regmi, S. Das, F. Hasan,

A. Tagge and I. M. Warner, Ionic liquid-based optoelectronic sensor arrays for chemical detection, *RSC Adv.*, 2014, **4**, 7225–7234.

2 P. Kipkorir and S. Magut, Ionic Liquids and GUMBOS for Biomedical and Sensing Applications, *LSU Dr. Diss.*, DOI:10.31390/gradschool_dissertations.718.

3 E. Krystkowiak, K. Dobek and A. Maciejewski, Origin of the strong effect of protic solvents on the emission spectra, quantum yield of fluorescence and fluorescence lifetime of 4-aminophthalimide: Role of hydrogen bonds in deactivation of S1-4-aminophthalimide, *J. Photochem. Photobiol. A Chem.*, 2006, **184**, 250–264.

4 H. Mohammad, A. S. M. Islam, C. Prodhan and M. Ali, A fluorescein-based chemosensor for "turn-on" detection of Hg 2+ and the resultant complex as a fluorescent sensor for S 2− in semi-aqueous medium with cell-imaging application: experimental and computational studies, *New J. Chem.*, 2019, **43**, 5297–5307.

5 T. Anand, G. Sivaraman and D. Chellappa, Hg2+ mediated quinazoline ensemble for highly selective recognition of Cysteine, *Spectrochim. Acta Part A Mol. Biomol. Spectrosc.*, 2014, **123**, 18–24.

6 S. Y. Moon, N. R. Cha, Y. H. Kim and S. K. Chang, New Hg2+-Selective Chromo- and Fluoroionophore Based upon 8-Hydroxyquinoline, *J. Org. Chem.*, 2004, **69**, 181–183.

7 F. Ye, X. M. Liang, K. X. Xu, X. X. Pang, Q. Chai and Y. Fu, A novel dithiourea-appended naphthalimide "on-off" fluorescent probe for detecting Hg2+ and Ag+ and its application in cell imaging, *Talanta*, 2019, **200**, 494–502.

8 R. Singh and G. Das, Fluorogenic detection of Hg2+ and Ag+ ions via two mechanistically discrete signal genres: A paradigm of differentially responsive metal ion sensing, *Sensors Actuators B Chem.*, 2018, **258**, 478–483.

9 S. Chen, W. Wang, M. Yan, Q. Tu, S. W. Chen, T. Li, M. Sen Yuan and J. Wang, 2-

Hydroxy benzothiazole modified rhodol: aggregation-induced emission and dual-channel fluorescence sensing of Hg2+ and Ag+ ions, *Sensors Actuators B Chem.*, 2018, **255**, 2086–2094.

10 J. H. Wang, Y. M. Liu, Z. M. Dong, J. Bin Chao, H. Wang, Y. Wang and S. M. Shuang, New colorimetric and fluorometric chemosensor for selective Hg2+ sensing in a near-perfect aqueous solution and bio-imaging, *J. Hazard. Mater.*, 2020, **382**, 121056.

11 Chethanakumar, M. Budri, K. B. Gudasi, R. S. Vadavi and S. S. Bhat, Luminescent Pyrene-based Schiff base Receptor for Hazardous Mercury(II) Detection Demonstrated by Cell Imaging and Test Strip, *J. Fluoresc.*, 2023, **33**, 539–551.

12 C. G. Chen, N. Vijay, N. Thirumalaivasan, S. Velmathi and S. P. Wu, Coumarin-based Hg2+ fluorescent probe: Fluorescence turn-on detection for Hg2+ bioimaging in living cells and zebrafish, *Spectrochim. Acta Part A Mol. Biomol. Spectrosc.*, 2019, **219**, 135–140.

13 L. Feng, W. Shi, J. Ma, Y. Chen, F. Kui, Y. Hui and Z. Xie, A novel thiosemicarbazone Schiff base derivative with aggregation-induced emission enhancement characteristics and its application in Hg2+ detection, *Sensors Actuators B Chem.*, 2016, **237**, 563–569.